

Published in final edited form as:

Nat Commun. 2011 ; 2: 251. doi:10.1038/ncomms1242.

Wwp2 is essential for palatogenesis mediated by the interaction between Sox9 and mediator subunit 25

Yukio Nakamura^{1,*}, Koji Yamamoto^{2,*}, Xinjun He³, Bungo Otsuki², Youngwoo Kim², Hiroki Murao², Tsunemitsu Soeda², Noriyuki Tsumaki⁴, Jian Min Deng⁵, Zhaoping Zhang⁵, Richard R. Behringer⁵, Benoit de Crombrughe⁵, John H. Postlethwait³, Matthew L. Warman⁶, Takashi Nakamura², and Haruhiko Akiyama²

¹Clinical Research Center, Murayama Medical Center, Tokyo 208-0011, Japan

²Department of Orthopaedics, Kyoto University, Kyoto 606-8507, Japan

³Institute of Neuroscience, University of Oregon, Eugene, Oregon 97403, USA

⁴Department of Bone and Cartilage Biology, Osaka University, Osaka 565-0871, Japan

⁵Department of Genetics, The University of Texas M.D. Anderson Cancer Center, Houston, Texas 77030, USA

⁶Howard Hughes Medical Institute, Department of Orthopaedic Surgery and Genetics, Children's Hospital and Harvard Medical School, Boston, Massachusetts 02115, USA

Abstract

Sox9 is a direct transcriptional activator of cartilage-specific extracellular matrix genes and has essential roles in chondrogenesis. Mutations in or around the *SOX9* gene cause campomelic dysplasia or Pierre Robin Sequence. However, *Sox9*-dependent transcriptional control in chondrogenesis remains largely unknown. Here we identify *Wwp2* as a direct target of Sox9. *Wwp2* interacts physically with Sox9 and is associated with Sox9 transcriptional activity via its nuclear translocation. A yeast two-hybrid screen using a cDNA library reveals that *Wwp2* interacts with Med25, a component of the Mediator complex. The positive regulation of Sox9 transcriptional activity by *Wwp2* is mediated by the binding between Sox9 and Med25. In zebrafish, morpholino-mediated knockdown of either *wwp2* or *med25* induces palatal malformation, which is comparable to that in *sox9* mutants. These results provide evidence that the regulatory interaction between Sox9, *Wwp2* and Med25 defines the Sox9 transcriptional mechanisms of chondrogenesis in the forming palate.

© 2011 Macmillan Publishers Limited. All rights reserved.

Correspondence and requests for materials should be addressed to H.A. (hakiyama@kuhp.kyoto-u.ac.jp).

*These authors contributed equally to this work.

Author contributions

H.A. directed the study; K.Y., B.O., Y.K., H.M., T.S., N.T. and T.N. performed all molecular and biochemical experiments; J.M.D., Z.Z., R.R.B. and B.d.C. generated mutant mice and performed the GeneChip analysis; and Y.N., X.H., J.H.P. and M.L.W. conducted all *in vivo* experiments.

Supplementary Information accompanies this paper at <http://www.nature.com/naturecommunications>

Competing financial interests: The authors declare no competing financial interests.

Accession codes: The microarray data have been deposited in ArrayExpress under the accession number E-MTAB-537.

The initiation of mesenchymal condensation and overt chondrogenesis depend on the transcription factor Sox9. Loss-of-function and gain-of-function analyses using mouse genetic approaches have revealed that Sox9 has an essential role in successive steps of chondrogenesis that are mediated by cell proliferation, differentiation and extracellular matrix production^{1,2}. Haploinsufficiency of *SOX9* causes campomelic dysplasia, which is a severe and often lethal skeletal dysplasia associated with sex reversal^{3,4}. Hypomorphic intragenic mutations or position effect translocation breakpoints around the *SOX9* gene cause the site- and stage-specific disruption of *SOX9* transcription, resulting in Pierre Robin Sequence⁵, which is characterized by micrognathis, glossoptosis and cleft palate. Indeed, heterozygous *Sox9* mutant mice died perinatally with cleft palate⁶. Previous studies have showed that Sox9 induces *L-Sox5* and *Sox6* transcription, and these Sox proteins coordinately regulate the expression of cartilage-specific extracellular matrix genes, including *Col2a1*, *Col11a2* and *Aggrecan*^{1,7-9}. Genetic variants in these genes also cause palatal malformation¹⁰⁻¹². These findings indicate that Sox9 transcriptional activity has a regulatory role in palatogenesis. The activity of Sox9 in chondrogenesis is controlled by several transcription factors. Recently, the thyroid hormone receptor-associated protein 230/Med12 (which is a member of the Mediator complex), the nuclear RNA-binding protein, p54^{nrb} the CREB-binding protein (CBP)/p300, and the Tat interactive protein-60 have been reported as modulators of Sox9 transcriptional activity¹³⁻¹⁷. However, Sox9-related genes and Sox9-dependent transcriptional regulation during chondrogenesis are not fully understood.

To define the repertoire of Sox9-dependent genes that contribute to the regulation of chondrogenesis, we generated Sox9-3' enhanced green fluorescent protein (EGFP) knock-in mice and Sox9-EGFP/EGFP null chimeras, and then performed a fluorescence-activated cell sorting (FACS)/comparative microarray gene expression analysis using EGFP-positive cells derived from limb buds of the mouse embryos. Subsequently, using *in situ* hybridization analysis of *Sox9* in limb buds of wild-type and conditional Sox9 knockout embryos harbouring the *Prx1-Cre* transgene, we identified genes that may be involved in chondrogenesis. Of these candidate genes, we focused on *Wwp2*, a member of the neural precursor cell expressed, developmentally downregulated 4-like protein family and the HECT domain E3 ubiquitin-protein ligases¹⁸. *Wwp2* controls the epithelial Na(+) channel¹⁹ and the divalent metal ion transporter DMT1²⁰. In addition, recent reports have showed that *Wwp2* mediates Oct4 ubiquitination and degradation in embryonic stem (ES) cells²¹. However, the expression and functions of *Wwp2* in chondrogenesis remain unknown.

Here we demonstrate that *Wwp2* interacts physically with Sox9 and Med25, mediator of RNA polymerase II transcription subunit 25, and reveal that Med25 transmits Sox9 transcriptional activity, which is mediated by binding with *Wwp2*. Furthermore, morpholino-mediated knockdown of either *wwp2* or *med25* induced palatal malformation in zebrafish, which is comparable to that observed in zebrafish *sox9* mutants. These findings provide new insights into the regulatory mechanisms of Sox9 transcriptional activity in chondrogenesis.

Results

***Wwp2* is identified as a *Sox9*-related gene in chondrogenesis**

To define the repertoire of *in vivo* *Sox9*-dependent genes in chondrogenesis, we performed FACS on genetically engineered mouse embryos that selectively express EGFP in a *Sox9*-specific pattern, followed by whole-genome microarray expression profiling on the isolated cells. For this purpose, we generated mutant mice in which an internal ribosome entry site (*IRES*)-EGFP-*pA/loxP*-flanked *PGK-neo-bpA* cassette was inserted into the 3'-untranslated region of the *Sox9* gene in exon 3 just at the 5' end to the polyadenylation signal (*Sox9*-3' EGFP knock-in mice; Fig. 1a,b). Heterozygous and homozygous *Sox9*-3' EGFP knock-in mice were viable and fertile and showed no noticeable phenotypic changes. In addition, EGFP expression was detectable in a *Sox9*-specific pattern during embryogenesis (Fig. 1c). Next, we generated *Sox9*-EGFP/EGFP null ES cells by insertion of *IRES-EGFP-pA/loxP*-flanked *PGK-neobpA* cassette into the coding regions of the *Sox9* gene (Fig. 1d–g). Our target strategy functionally inactivated *Sox9* and led to the expression of EGFP in a *Sox9*-specific pattern.

The purity of EGFP-positive cells of *Sox9*-3' EGFP knock-in and *Sox9*-EGFP/EGFP null chimeric embryos harvested from limb buds at embryonic day 12.5 (E12.5) was 96.0 and 94.8%, respectively (Fig. 1h), and reverse transcription (RT)-PCR analysis revealed that the expression of *Sox9* in the majority of the population of cells isolated from *Sox9*-EGFP/EGFP null chimeras was deleted (Fig. 1i). Following the first screening of the microarray analysis (the complete annotated data set is available from the ArrayExpress repository, accession number E-MTAB-537), we further narrowed down the *Sox9*-related candidate genes using *in situ* hybridization in limb buds of E12.5 wild-type and conditional *Sox9* knockout embryos harbouring the *Prx1-Cre* transgene. With the exception of *Sox5*, *Sox6*, *Col2a1*, *Col9a1*, *Col9a3* and *Col11a1*, 27 genes that exhibited the same pattern as *Sox9* in conditional *Sox9* knockout embryos were identified as *Sox9*-related genes involved in chondrogenesis (Supplementary Table S1). *Wwp2* showed 6.24-fold change in mRNA expression.

Wwp2* is a downstream target of *Sox9

The mRNA of *Wwp2* is expressed in various adult mouse tissues, whereas *Sox9* mRNA is detected in specific tissues (Supplementary Fig. S1a,b). During limb bud development in mouse embryos, *Wwp2* was expressed during mesenchymal condensations of limb buds at E12.5, and then in periarticular and proliferating chondrocytes at E16.5 (Fig. 2a). These expression patterns of *Wwp2* during chondrogenesis coincided with that of *Sox9*. The expression of *Wwp2* mRNA was completely abolished by the conditional inactivation of *Sox9* using *Prx1-Cre*-mediated recombination in the limbs at E12.5 and *Col2a1-Cre*-mediated recombination in chondrocytes at E16.5 (Fig. 2a). Furthermore, adenoviral overexpression of *Sox9* in ATDC5 cells, a clonal murine chondrogenic cell line, induced the upregulation of *Wwp2* significantly (Fig. 2b); in contrast, knockdown of *Sox9* using short interfering RNA (siRNA) led to significant downregulation of its expression (Fig. 2b), and the expression of *Wwp2* protein also showed a *Sox9* dependency (Supplementary Fig.

S1c,d). Thus, these results indicate that *Wwp2* is a downstream target of *Sox9*, *in vivo* and *in vitro*.

Wwp2 transcription is regulated directly by Sox9

Next, we assessed whether *Sox9* regulates the transcription of *Wwp2* directly. Putative *Sox9*-binding sites in the *Wwp2* promoter region that are highly conserved among mammals (human, rat and mouse) were examined using *in silico* homology searches. A search of the region up to 4,000 nucleotides (nt) of *Wwp2* exon 1 identified a putative *Sox9*-binding sequence (ACAAAGG), which lies between nt – 529 and – 523 and includes a nearly consensus motif for the *Sox9*-specific DNA-binding element²². To clarify the activity of the putative *Sox9*-responsive element of the *Wwp2* promoter, a luciferase reporter assay was performed using a series of truncated fragments of the *Wwp2* promoter cloned into a luciferase reporter vector (Fig. 2c). The results showed that co-transfection of pW_{–790} (which contains the *Wwp2* promoter region from nt – 790 to – 64) and a *Sox9* expression vector into HEK293 cells induced an approximately twofold increase in the relative reporter activity compared with that observed for the control (Fig. 2c). In addition, this increase in reporter activity was mostly abolished by using the mutated pW_{–790} (termed pWM_{–790}) or pW_{–391} (which lacked the putative *Sox9*-binding motif). To obtain direct evidence of *Sox9*-mediated binding to this site, a chromatin immunoprecipitation (ChIP) assay was performed. The ChIP experiment using adenoviruses expressing *Sox9* in ATDC5 cells detected the specific binding of *Sox9* to the endogenous *Wwp2* promoter element (Fig. 2d). Moreover, an electrophoretic mobility shift assay (EMSA) provided further evidence that HA-tagged *Sox9* bound to the DNA fragment of this site (Fig. 2e). Hence, we conclude that *Sox9* binds to the *Wwp2* promoter element directly and transactivates *Wwp2* expression.

wwp2 knockdown induces palatal malformation in zebrafish

In zebrafish, the expression of *wwp2* in the cartilage of pharyngeal arches at 3 days post fertilization (dpf) was strongly reduced in embryos that were homozygous for *sox9a* or *sox9b* mutations (Supplementary Fig. S2a), whereas its expression in wild-type pharyngeal arches was detected at 2 dpf (Supplementary Fig. S2b). Interestingly, morpholino-mediated knockdown of *wwp2* resulted in a small and fused palate, a phenotype that was reminiscent of *sox9*-mutant zebrafish (Fig. 2f)²³; however, the expression of *sox9a* and *sox9b*, as detected in RT-PCR experiments, did not change after downregulation of *wwp2* expression (Supplementary Fig. S2c). Furthermore, the co-injection of both *sox9a* and *sox9b* mRNA together with *wwp2* morpholinos could partially rescue the palatal malformation (Fig. 2g,h). This restoration was thought to be due to the exogenous *sox9*-dependent induction of endogenous *wwp2* expression. These findings would be expected under the hypothesis that *Wwp2* has an essential role in chondrogenesis during palatogenesis, as an *in vivo* direct target of *Sox9*.

Wwp2 interacts physically with Sox9

The similar palatal phenotype observed in *sox9a*-, *sox9b*- and *wwp2*-deficient zebrafish raises the possibility of physical and functional interactions between *Sox9* and *Wwp2*. An IP experiment of endogenous *Sox9* and myc-tagged *Wwp2* using ATDC5 cells showed that

Sox9 physically interacted with Wwp2 (Fig. 3a). Co-IP experiments using deletion mutations of *Sox9* (Fig. 3b) and *Wwp2* (Fig. 3c) showed that the binding between Sox9 and Wwp2 was mediated by the carboxy terminal transactivation domain of Sox9 (Fig. 3d) and by the amino terminus (N-terminus) of Wwp2 (Fig. 3e), and not by the WW domains, which have a direct role in the mediation of specific and distinct interactions with Wwp2 substrates²⁴. Indeed, Wwp2 did not stimulate ubiquitylation-mediated Sox9 degradation (Supplementary Fig. S3).

Wwp2 promotes the transcriptional activity of Sox9

To elucidate whether Wwp2 is associated with Sox9 transcriptional activity, we investigated the nuclear localization of Wwp2 in chondrocytes, the nuclear translocation of Wwp2 in the presence or absence of exogenously expressed Sox9, and then performed luciferase reporter assays using a chondrocyte-specific p89/4×48 *Col2a1* reporter and a *Coll1a2* reporter construct. Immunohistochemical staining exhibited the abundant nuclear localization of Sox9 and Wwp2 in proliferating and pre-hypertrophic chondrocytes of mouse limb buds at E16.5 (Fig. 3f). Interestingly, *in vitro* multiple immunofluorescence (IF) of C3H10T1/2 cells, mouse pluripotent embryonic mesenchymal cell lines, co-transfected with HA-tagged *Sox9* and/or myc-tagged *Wwp2* revealed that the exogenously expressed Sox9 induced nuclear translocation of Wwp2 (Fig. 3g and Supplementary Fig. S4 for lower magnification image). This result indicates that Sox9 mediates the recruitment of Wwp2 from the cytosol into the nucleus in chondrocytes. Furthermore, *Wwp2* co-transfected with *Sox9* into C3H10T1/2 cells enhanced the *Col2a1* and *Coll1a2* reporter activities in a dose-dependent manner (Fig. 3h). Thus, these results strongly suggest that Wwp2 promotes the transcriptional activity of Sox9 as a cofactor in the nucleus of chondrocytes.

Wwp2 binds to Med25 in chondrocytes

To identify the mechanism underlying the Wwp2-mediated promotion of Sox9 transcriptional activity in chondrocytes, we sought other Wwp2-interacting proteins directly in chondrocytes using a yeast two-hybrid screening approach and identified Med25. Med25 exhibited strong physical interaction with Wwp2 in yeast (Fig. 4a). The mRNA of *Med25* was expressed in various adult mouse tissues (Supplementary Fig. S5), and Med25 was detected in mouse limb bud chondrocytes at E16.5 (Fig. 4b). Med25 was reported as a specific target of the VP16 transcriptional activator²⁵, and was shown to enhance retinoic acid receptor/retinoid X receptor-mediated transcription in co-operation with CBP and mediators²⁶. In addition, in human disease, homozygous mutation of *MED25* is responsible for Charcot–Marie–Tooth syndrome type 2B²⁷. However, the molecular functions of Med25 in chondrogenesis remain unknown.

med25 knockdown induces palatal malformation in zebrafish

To clarify the role of Med25 in chondrogenesis, we investigated the *in vivo* functions of Med25 for skeletal formation in zebrafish. *In situ* hybridization showed that *med25* was broadly expressed in the head, body and tail at 1 and 2 dpf (Fig. 4c). Intriguingly, morpholino-mediated knockdown of *med25* in zebrafish resulted in palatal malformation (Fig. 4d), which closely resembled the palatal phenotype of *wwp2* or *sox9* mutants²³ (Fig.

2f). Furthermore, these palatal malformations could not be rescued by the co-injection of *sox9a* and *sox9b* mRNA or *wwp2* mRNA (Supplementary Fig. S6a,b). Also, the injection of *med25* mRNA with the *wwp2* morpholinos had no influence on the palatal phenotype (Supplementary Fig. S6c). These findings suggest that Med25 transmits Sox9 transcriptional activity to general transcription machinery in association with Wwp2 in palatogenesis.

Med25 interacts physically with Sox9 and Wwp2

The *in vivo* phenotypic similarities in palatogenesis between the knockdown of *Sox9*, *Wwp2* and *Med25*, and the mutual interactions of Wwp2 with Sox9 and Med25, strongly suggest a functional communication between Sox9 and Med25 during chondrogenesis. Therefore, to assess whether Sox9 interacts physically and/or functionally with Med25, an IP assay was performed using ATDC5 cells transfected with HA-tagged *Med25*. The result showed that Med25 interacted physically with endogenous Sox9 (Fig. 4e). Co-IP experiments using deletion mutations of *Sox9*, *Wwp2* and *Med25* (Figs 3b,c and 4f) led to the following results. First, Med25 interacted physically with the N-terminus of Wwp2 and Wwp2 bound to the PTOV domain of Med25, which includes its transactivation domain²⁶ (Fig. 4g,h), and not to the SD1 domain of Med25, which contains the putative PY motif (the WW domains of Wwp2 have a preference for the PY motif in the binding of substrate proteins)^{28,29}. Indeed, Wwp2 did not stimulate ubiquitylation-mediated Med25 degradation (Supplementary Fig. S7). Second, Med25 and Sox9 interacted with each transactivation domain (Fig. 4i,j). Thus, these physical interactions between Sox9, Wwp2 and Med25 suggest their functional interactions. In addition, multiple IF experiments revealed that Med25 was expressed in cell nucleus, and the nuclear translocation of Wwp2 depended on Sox9 and not on Med25 (Supplementary Fig. S8a,b).

Wwp2 and Med25 augment Sox9 transcriptional activity

Luciferase reporter assays using the p89/4×48 *Col2a1* reporter or the *Col11a2* reporter showed that co-transfection with *Sox9*, *Wwp2* and *Med25* enhanced reporter activity significantly compared with that observed for *Sox9* and *Wwp2* or for *Sox9* and *Med25* (Fig. 5a). Interestingly, *Wwp2* carrying a mutation in the HECT domain, which leads to loss of its catalytic function as an E3 ligase (*Wwp2-CA*; change of the cysteine residue at position 838 to an alanine), was still capable of increasing Sox9-dependent *Col2a1* and *Col11a2* luciferase activity (Fig. 5a). However, the slightly lower luciferase activity observed when using *Wwp2-CA* would indicate a loss of ubiquitylation-dependent activation by other molecules that regulate the transcription of *Col2a1* and *Col11a2*. Knockdown of either *Wwp2* or *Med25* in C3H10T1/2 cells resulted in significant downregulation of *Col2a1* transcripts (Fig. 5b,c). In addition, this *in vitro* downregulation was not restored by adenoviral overexpression of Sox9 (Fig. 5d), which strongly suggests that Wwp2 and Med25 are key mediators of Sox9-dependent transcription.

Wwp2 forms a transcriptional complex with Sox9 and Med25

To obtain direct evidence of the formation of transcriptional complex through binding of these proteins to the chondrocyte-specific enhancer of the *Col2a1* gene, we performed EMSA and ChIP assays using C3H10T1/2 cells, and revealed that Sox9, Wwp2 and Med25

were recruited onto the *Col2a1* enhancer as a transcriptional complex (Fig. 5e,f). Importantly, knockdown of *Wwp2* in ATDC5 cells attenuated the physical interaction between endogenous Sox9 and HA-tagged Med25 (Fig. 5g). Thus, these results indicate that *Wwp2* mediates the interaction between Sox9 and Med25 via mutual physical binding and regulates Sox9 transcriptional activity.

Discussion

Here we identified *Wwp2* as a Sox9 downstream target using FACS/microarray gene expression analysis and confirm the findings by *in situ* hybridization in conditional Sox9 knockout embryos and overexpression and knockdown of Sox9 in *in vitro* cells. Furthermore, both EMSA and ChIP assays using an anti-Sox9 antibody and reporter assays with luciferase reporter constructs indicate that Sox9 binds to the *Wwp2* promoter and regulates *Wwp2* expression directly. Zou *et al.*³⁰ recently reported that *Wwp2* is detected in cartilaginous regions of the skull that are also positive for Sox9 and that Sox9 binds to an intronic region of *Wwp2*, which mediates the Sox9- dependent expression of *Wwp2*. Thus, these findings indicate that Sox9 regulates the cartilaginous expression of *Wwp2* directly.

Palatogenesis is controlled by multiple genetic factors, including genes encoding extracellular matrix proteins, growth factors and cell adhesion molecules. Alterations in the synthesis and accumulation of extracellular matrix proteins, including type II, IX, XI collagens, and proteoglycan¹⁰⁻¹² impair palatogenesis, all of that are regulated by Sox9^{1,7-9}. Indeed, mutations in or around *SOX9* gene result in palatal malformations in human and a mouse model. Thus, it is obvious that Sox9 has a crucial role in palatogenesis. In this study, we show that *Wwp2* is required for palatogenesis, mediated by formation of a transcriptional complex with Sox9 and Med25. Morpholino-mediated knockdown of *wwp2* in zebrafish results in palatal malformation, which is comparable to that in *Wwp2*- deficient mice reported by Zou *et al.*³⁰ They also show that *Wwp2* interacts with Goosecoid to facilitate its monoubiquitylation and augments its transcriptional activity for Sox6 expression³⁰. Taking together with the previous findings that Sox6 cooperates with Sox9 to directly activate downstream target genes encoding extracellular matrix proteins^{7,8}, it is likely that *Wwp2* is essential for palatogenesis through Sox9 transcriptional activity (as shown in Fig. 5h).

Because Sox9 is required for the development of several tissues, which are characterized by very different genetic programs, other transcription factors and coactivators should provide specificity to the function of Sox9 in each of these cell types. Transcription factors form a large complex including the Mediator complex that conveys regulatory information from enhancer elements to the basal transcription machinery and acts as a bridge between transcription factors and RNA polymerase II. A recent study using human hepatocytes shows that Med25 is required for the recruitment of RNA polymerase II to the promoter of hepatocyte nuclear factor 4 α and interacts with hepatocyte nuclear factor 4 α through its transactivation domain³¹. Hence, it is likely that Med25 recruits RNA polymerase II on the promoter of Sox9 target genes. Med25 is believed to function in chromatin modification and pre-initiation complex assembly by recruiting CBP and the Mediator complex²⁶. In addition, Trap230/Med12 is known as a coactivator of Sox9- dependent transcriptional regulation¹⁴. The phenotypic similarity in palatogenesis among *sox9a/sox9b*, *wwp2*, *med25* and *Trap230/*

med12 mutants^{14,23} and the *in vitro* physical interaction between Sox9/Trap230, Sox9/Med25, Sox9/Wwp2 and Wwp2/Med25 may reflect a possible regulatory axis, which would include a Sox9–Wwp2–Med25–Trap complex.

In conclusion, Sox9 stimulates *Wwp2* expression and induces the translocation of Wwp2 into the nucleus of chondrocytes. Wwp2 mediates the binding between Sox9 and Med25, resulting in transactivation of target genes (Fig. 5h). This molecular mechanism is thought to be involved in palatogenesis *in vivo*. Our findings provide new insights into the regulatory mechanisms of Sox9 transcriptional activity during chondrogenesis and suggest new ideas regarding the molecular basis of the pathogenesis of cleft palate.

Methods

Mice

Sox9-3' EGFP knock-in mice were generated using the targeting vector that spanned a 7.7 kb fragment of the mouse 129SvEv *Sox9* gene³². An *IRES-EGFPpA/loxP-flanked PGK-neo-bpA* cassette was inserted into an HpaI site within the 3'-untranslated region in exon 3. The targeting vector was introduced into PC3 mouse ES cells. Mouse chimeras were generated by injection of mutant ES cell clones into C57BL/6 host blastocysts; the resulting chimeras were bred with C57BL/6 mice to generate Sox9-3' EGFP knock-in heterozygous mice.

Sox9-EGFP/EGFP null chimeras were generated using a 4.5 kb NotI–SacII 5' fragment and a 2.5 kb SacI–SacI 3' fragment derived from the *Sox9* locus³³. An *IRES-EGFP-pA/loxP-flanked PGK-neo-bpA* cassette was introduced into the first exon of *Sox9*, simultaneously deleting the translation start site and a portion of the high-mobility group DNA-binding domain. The targeting vector was introduced into AB-1 ES cells. To reuse G418 selection, the *loxP-flanked neo* cassette was excised from the Sox9 EGFP-neo/ + ES cell lines by transient expression of Cre recombinase. Neo-deleted Sox9 EGFP/ + ES cell clones were identified by Southern blot and verified by G418 selection. The Sox9 EGFP/ + ES cell lines were then retargeted with the original vector, as described above, and Sox9-EGFP/EGFP null ES cells were verified by Southern blot. The Sox9-EGFP/EGFP null ES cells were microinjected into C57BL/6 mouse blastocysts to generate chimeric embryos. Experimental procedures and animal maintenance followed institutional guidelines and were approved by local authorities.

FACS and microarray analysis

The limb buds of E12.5 Sox9-3' EGFP knock-in and Sox9-EGFP/EGFP null chimeric embryos were dissected and dissociated into single cells using collagenase and disperse digestion. EGFP-positive cells were sorted using a FACSAria flow cytometer (Becton-Dickinson). Deletion of *Sox9* in the cells harvested from Sox9-EGFP/EGFP null chimeric embryos was verified by PCR (Supplementary Table S2). Total RNA was extracted and amplified according to the instructions provided by Affymetrix. Microarray analysis using the Affymetrix Mouse Genome 430 2.0 Array was performed according to the manufacturer's instructions.

***In situ* hybridization of mouse embryos**

The development-associated expression patterns of *Sox9* and *Wwp2* mRNA in the limb buds of wild-type, *Sox9^{flox/flox}Prrx1-Cre* and *Sox9^{flox/flox}Col2a1-Cre* embryos were analysed using the hybridization probes for *Sox9* (255 bp) and *Wwp2* (440 bp).

Yeast two-hybrid screen

A yeast two-hybrid assay was carried out using Matchmaker Library Construction & Screening Kits (Clontech), according to the manufacturer's instructions. The full-length mouse *Wwp2* cDNA inserted into pGBKT7 was used as the bait vector. Med25 identified using a cDNA library from mouse rib chondrocytes was inserted into pGADT7 (prey vector). The pGADT7 vector expressing full-length Med25 was retransformed into the AH109 yeast strain, together with the pGBKT7 vector expressing *Wwp2* or with the pGBKT7-Lam vector (negative control), and cultured on SD/– Ade/– His/– Leu/– Trp/ X- α -Gal high-stringency plates.

Zebrafish

Developing and adult zebrafish were maintained using standard methods. Wild-type matings were obtained from the Oregon AB line. To suppress pigmentation, embryos were raised in zebrafish aquatic system water containing 1-phenyl-2-thiourea (0.003%) (Sigma). Zebrafish care was in accordance with the guidelines of the Children's Hospital Boston, University of Oregon and Murayama Medical Center.

***In situ* hybridization of zebrafish**

Whole-mount *in situ* hybridization was carried out in zebrafish embryos at 1 and 2 dpf. Digoxigenin-labelled RNA probes were generated using the T7 and T3 labelling kit (Roche), according to the manufacturer's instructions. Signals were detected with an alkaline phosphatase-conjugated anti-digoxigenin antibody (Roche) and 4-nitro blue tetrazolium and 5-bromo-4-chloro-3-indolyl-phosphate. The primer sequences of the probes were described in Supplementary Table S2.

Morpholino knockdown and RNA rescue in zebrafish

Gene Tools (Philomath; <http://www.gene-tools.com>) supplied morpholino oligonucleotides (MOs) with the sequences: zebrafish *wwp2* splice blocker-MO, 5'-CAGTGTGAATGCAGTGT TTT ACCCA-3' and zebrafish *med25* ATG blocker, 5'-TATGGGTCACCTTTGGTCT ACAGCC-3'. We injected one- or two-cell stage zebrafish embryos with ~1–2 nl of morpholinos (20–25 ng for *wwp2* splice blocker-MO and 5–10 ng for *med25* ATG blocker). In RNA rescue experiments, we performed a series of experiments injecting each morpholino with either 50–500 pg of *sox9a* and/or *sox9b*, *wwp2* or *med25* mRNA.

Zebrafish cartilage staining

Zebrafish embryos at 4–7 dpf were stained with alcian blue and alizarin red and were flat mounted³⁴. Images of stained, flat-mounted cartilages were captured using a Leica DMLB upright microscope and Spot camera (Diagnostic Instruments, Inc).

siRNA

The mouse *Sox9*-specific siRNA (MISSION siRNA) was purchased from Sigma-Aldrich and the mouse *Wwp2*- and *Med25*-specific siRNAs (ON-TARGET plus SMARTpool) were purchased from Thermo Scientific Dharmacon. For mRNA expression analysis, each siRNA construct was transfected individually into ATDC5 or C3H10T1/2 cells (final concentration 150 nM) according to the manufacturer's protocol. Total RNA was extracted 48 h after transfection. A total of 1 µg of total RNA was used to synthesize cDNA using the Transcriptor First-Strand cDNA Synthesis Kit (Roche). Quantitative RT-PCR was performed using a LightCycler Instrument and a LightCycler FastStart DNA Master SYBR Green 1 Kit (Roche). The primer sequences for quantitative RT-PCR were described in Supplementary Table S2.

Luciferase assays

In promoter analysis, mouse *Wwp2* promoter fragments located upstream of the 5'-flanking region of exon 1 (-1,172 bp to -64 bp, -790 bp to -64 bp, and -391 bp to -64 bp) were subcloned into the pGL3-basic vector (Promega) to generate the *Wwp2* promoter/luciferase reporter constructs, designated pW₋₁₁₇₂, pW₋₇₉₀ and pW₋₃₉₁, respectively. The mutated pW₋₇₉₀ (termed pWM₋₇₉₀) construct, which includes a 2 bp substitution mutation in the nearly consensus binding site for high-mobility group box proteins, was produced using the QuickChange site-directed mutagenesis kit (Stratagene), according to the manufacturer's protocol. In *Col2a1* or *Col11a2* reporter analysis, a chondrocyte-specific p89/4×48 *Col2a1* reporter or a *Col11a2-luc* reporter construct was used. pcDNA-renilla luciferase was used as an internal control. The plasmids were transfected using the FuGene HD transfection reagent (Roche) into HEK293 or C3H10T1/2 cells. Luciferase activity was assayed 48 h after transfection, according to the manufacturer's instructions.

ChIP

ChIP assays were performed using the ChIP Kit (Abcam), according to the manufacturer's protocol. ATDC5 cells cultured in six-well plates were infected with adenoviruses expressing Sox9; 48 h after infection, the fragments of cross-linked chromatin were immunoprecipitated with 3 µg of rabbit IgG (Cell signaling, 1 mg ml⁻¹) or anti-Sox9 antibody (Chemicon, 1 mg ml⁻¹). PCR primers were designed to contain a putative binding site within the mouse *Wwp2* promoter region (Supplementary Table S2). C3H10T1/2 cells were co-transfected with Flag-tagged Sox9, 6× myc-tagged *Wwp2* and 3× HA-tagged *Med25* expression vectors, and ChIP assay was performed according to the same scheme using 3 µg of anti-Flag (Abcam, 1 mg ml⁻¹), anti-myc (Abcam, 1 mg ml⁻¹) and anti-HA (Santa Cruz, 1 mg ml⁻¹) antibodies. PCR was performed to detect the co-precipitation of the *Col2a1* enhancer region (Supplementary Table S2).

EMSA

A DNA probe corresponding to the putative Sox9 binding sequence of the 5'-flanking region of the *Wwp2* gene was prepared by annealing complementary oligonucleotides (Supplementary Table S2). The Sox9 protein was synthesized *in vitro* using a transcription/translation system (Promega). DNA-binding reactions and EMSA with the 48 bp *Col2a1*

enhancer probe were performed using nuclear proteins of C3H10T1/2 cells co-transfected with 6× myc-tagged Wwp2 and 3× HA-tagged Med25 expression vectors³⁵ (Supplementary Table S2).

Immunoprecipitation

Tagged plasmids were transfected into ATDC5, C3H10T1/2 or HEK293 cells, and after 48 h, cells were lysed in buffer (50 mM Tris, 150 mM NaCl, 1 mM EDTA and 1% Triton X-100). Protein complexes were immunoprecipitated using protein G agarose with 3 µg of anti-Sox9 antibody (Chemicon, 1 mg ml⁻¹), 3 µg of anti-V5 antibody (MBL, 1 mg ml⁻¹), 30 µl of Ezview Red ANTI-FLAG M2 Affinity Gel (Sigma) or 30 µl of Anti-HA Affinity Matrix (Roche). Immunoprecipitated proteins were analysed by immunoblotting using each antibody.

Immunohistochemical analysis

Mouse limb buds at E16.5 were fixed in 4% paraformaldehyde and embedded in paraffin. Immunohistochemical analysis was performed using 3,3'-diaminobenzidine (DAB) staining (Zymed), and hematoxylin was used as a counterstain. The following primary antibodies were used: goat polyclonal anti-Sox9 antibody (Santa Cruz, 0.2 mg ml⁻¹), rabbit polyclonal anti-AIP2 antibody (Santa Cruz, 0.2 mg ml⁻¹) and goat polyclonal anti-Med25 antibody (Santa Cruz, 0.2 mg ml⁻¹) diluted in antibody diluent (Zymed) to 1:100.

IF staining

IF staining was performed using C3H10T1/2 cells. Cells were fixed and permeabilized with cold methanol for 25 min at 4 °C. After washing, cells were blocked with a fresh blocking solution (4% donkey serum in PBS containing 0.05% Tween-20 (PBST)) for 30 min and were incubated with a rabbit anti-HA antibody (Santa Cruz, 0.2 mg ml⁻¹) diluted to 1:200 in 1% donkey serum/PBS containing 0.05% Tween-20 for 1 h at room temperature. Cells were washed and incubated with an fluorescein isothiocyanate-conjugated donkey anti-rabbit IgG antibody (Jackson ImmunoResearch Laboratories, 0.5 mg ml⁻¹), diluted to 1:1,000 for 1 h at room temperature. After washing, the procedure used for multiple staining was repeated using a goat anti-myc antibody (Abcam, 1 mg ml⁻¹) or a goat anti-Flag antibody (Abcam, 1 mg ml⁻¹; 1:200), and a TRITC-conjugated donkey anti-goat IgG antibody (1:1,000; Jackson ImmunoResearch Laboratories, 0.5 mg ml⁻¹). Confocal images were obtained with a confocal laser microscope (Nikon Instruments Inc.).

Statistical analysis

Statistical evaluation was conducted using the Student's *t*-test or Dunnett's test. All error bars represent s.d. and significance was assessed as $P < 0.05$.

Supplementary Material

Refer to Web version on PubMed Central for supplementary material.

Acknowledgments

We thank Andreas Schedl, Stephen O’Gorman and James F. Martin for valuable help. These studies were supported by a Grant-in-aid for Scientific Research from the Japanese Ministry of Education, Culture, Sports, Science, and Technology (#20659231), a Takeda Science Foundation grant to H.A., a National Institutes of Health HD30284 grant to R.R.B. and National Institutes of Health grants HD022486 and DE020076 to J.H.P.

References

1. Akiyama H, Chaboissier MC, Martin JF, Schedl A, de Crombrugge B. The transcription factor Sox9 has essential roles in successive steps of the chondrocyte differentiation pathway and is required for expression of Sox5 and Sox6. *Genes Dev.* 2002; 16:2813–2828. [PubMed: 12414734]
2. Akiyama H, et al. Interactions between Sox9 and beta-catenin control chondrocyte differentiation. *Genes Dev.* 2004; 18:1072–1087. [PubMed: 15132997]
3. Wagner T, et al. Autosomal sex reversal and campomelic dysplasia are caused by mutations in and around the SRY-related gene SOX9. *Cell.* 1994; 79:1111–1120. [PubMed: 8001137]
4. Foster JW, et al. Campomelic dysplasia and autosomal sex reversal caused by mutations in an SRY-related gene. *Nature.* 1994; 372:525–530. [PubMed: 7990924]
5. Benko S, et al. Highly conserved non-coding elements on either side of SOX9 associated with Pierre Robin sequence. *Nat Genet.* 2009; 41:359–364. [PubMed: 19234473]
6. Bi W, et al. Haploinsufficiency of Sox9 results in defective cartilage primordia and premature skeletal mineralization. *Proc Natl Acad Sci USA.* 2001; 98:6698–6703. [PubMed: 11371614]
7. Smits P, et al. The transcription factors L-Sox5 and Sox6 are essential for cartilage formation. *Dev Cell.* 2001; 1:277–290. [PubMed: 11702786]
8. Lefebvre V, Li P, de Crombrugge B. A new long form of Sox5 (L-Sox5), Sox6 and Sox9 are coexpressed in chondrogenesis and cooperatively activate the type II collagen gene. *EMBO J.* 1998; 17:5718–5733. [PubMed: 9755172]
9. Han Y, Lefebvre V. L-Sox5 and Sox6 drive expression of the *aggrecan* gene in cartilage by securing binding of Sox9 to a far-upstream enhancer. *Mol Cell Biol.* 2008; 28:4999–5013. [PubMed: 18559420]
10. Nikopensius T, et al. Genetic variants in COL2A1, COL11A2, and IRF6 contribute risk to nonsyndromic cleft palate. *Birth Defects Res A Clin Mol Teratol.* 2010; 88:748–756. [PubMed: 20672350]
11. Melkonieni M, et al. Collagen XI sequence variations in nonsyndromic cleft palate, Robin sequence and micrognathia. *Eur J Hum Genet.* 2003; 11:265–270. [PubMed: 12673280]
12. Watanabe H, et al. Mouse cartilage matrix deficiency (*cmd*) caused by a 7 bp deletion in the *aggrecan* gene. *Nat Genet.* 1994; 7:154–157. [PubMed: 7920633]
13. Tsuda M, Takahashi S, Takahashi Y, Asahara H. Transcriptional co-activators CREB-binding protein and p300 regulate chondrocyte-specific gene expression via association with Sox9. *J Biol Chem.* 2003; 278:27224–27229. [PubMed: 12732631]
14. Rau MJ, Fischer S, Neumann CJ. Zebrafish Trap230/Med12 is required as a coactivator for Sox9-dependent neural crest, cartilage and ear development. *Dev Biol.* 2006; 296:83–93. [PubMed: 16712834]
15. Zhou R, et al. SOX9 interacts with a component of the human thyroid hormone receptor-associated protein complex. *Nucleic Acids Res.* 2002; 30:3245–3252. [PubMed: 12136106]
16. Hata K, et al. Paraspeckle protein p54nrb links Sox9-mediated transcription with RNA processing during chondrogenesis in mice. *J Clin Invest.* 2008; 118:3098–3108. [PubMed: 18677406]
17. Hattori T, et al. Transcriptional regulation of chondrogenesis by coactivator Tip60 via chromatin association with Sox9 and Sox5. *Nucleic Acids Res.* 2008; 36:3011–3024. [PubMed: 18390577]
18. Rotin D, Kumar S. Physiological functions of the HECT family of ubiquitin ligases. *Nat Rev Mol Cell Biol.* 2009; 10:398–409. [PubMed: 19436320]
19. McDonald FJ, et al. Ubiquitin-protein ligase WWP2 binds to and downregulates the epithelial Na(+) channel. *Am J Physiol Renal Physiol.* 2002; 283:F431–436. [PubMed: 12167593]

20. Foot NJ, et al. Regulation of the divalent metal ion transporter DMT1 and iron homeostasis by a ubiquitin-dependent mechanism involving Ndfips and WWP2. *Blood*. 2008; 112:4268–4275. [PubMed: 18776082]
21. Xu HM, et al. Wwp2, an E3 ubiquitin ligase that targets transcription factor Oct-4 for ubiquitination. *J Biol Chem*. 2004; 279:23495–23503. [PubMed: 15047715]
22. Mertin S, McDowall SG, Harley VR. The DNA-binding specificity of SOX9 and other SOX proteins. *Nucleic Acids Res*. 1999; 27:1359–1364. [PubMed: 9973626]
23. Yan YL, et al. A pair of Sox: distinct and overlapping functions of zebrafish sox9 co-orthologs in craniofacial and pectoral fin development. *Development*. 2005; 132:1069–1083. [PubMed: 15689370]
24. Macias MJ, et al. Structure of the WW domain of a kinase-associated protein complexed with a proline-rich peptide. *Nature*. 1996; 382:646–649. [PubMed: 8757138]
25. Yang F, DeBeaumont R, Zhou S, Naar AM. The activator-recruited cofactor/Mediator coactivator subunit ARC92 is a functionally important target of the VP16 transcriptional activator. *Proc Natl Acad Sci USA*. 2004; 101:2339–2344. [PubMed: 14983011]
26. Lee HK, Park UH, Kim EJ, Um SJ. MED25 is distinct from TRAP220/MED1 in cooperating with CBP for retinoid receptor activation. *EMBO J*. 2007; 26:3545–3557. [PubMed: 17641689]
27. Leal A, et al. Identification of the variant Ala335Val of MED25 as responsible for CMT2B2: molecular data, functional studies of the SH3 recognition motif and correlation between wild-type MED25 and PMP22 RNA levels in CMT1A animal models. *Neurogenetics*. 2009; 10:275–287. [PubMed: 19290556]
28. Martin-Serrano J, Eastman SW, Chung W, Bieniasz PD. HECT ubiquitin ligases link viral and cellular PPXY motifs to the vacuolar protein-sorting pathway. *J Cell Biol*. 2005; 168:89–101. [PubMed: 15623582]
29. Murillas R, Simms KS, Hatakeyama S, Weissman AM, Kuehn MR. Identification of developmentally expressed proteins that functionally interact with Nedd4 ubiquitin ligase. *J Biol Chem*. 2002; 277:2897–2907. [PubMed: 11717310]
30. Zou W, et al. The E3 ubiquitin ligase Wwp2 regulates craniofacial development through mono-ubiquitylation of Goosecoid. *Nat Cell Biol*. 2010; 13:59–65. [PubMed: 21170031]
31. Rana R, Surapureddi S, Kam W, Ferguson S, Goldstein JA. Med25 is required for RNA polymerase II recruitment to specific promoters, thus regulating xenobiotic and lipid metabolism in human liver. *Mol Cell Biol*. 2011; 31:466–481. [PubMed: 21135126]
32. Akiyama H, et al. Osteo-chondroprogenitor cells are derived from Sox9 expressing precursors. *Proc Natl Acad Sci USA*. 2005; 102:14665–14670. [PubMed: 16203988]
33. Bi W, Deng JM, Zhang Z, Behringer RR, de Crombrughe B. Sox9 is required for cartilage formation. *Nat Genet*. 1999; 22:85–89. [PubMed: 10319868]
34. Walker MB, Kimmel CB. A two-color acid-free cartilage and bone stain for zebrafish larvae. *Biotech Histochem*. 2007; 82:23–28. [PubMed: 17510811]
35. Lefebvre V, Huang W, Harley VR, Goodfellow PN, de Crombrughe B. SOX9 is a potent activator of the chondrocyte-specific enhancer of the pro alpha1(II) collagen gene. *Mol Cell Biol*. 1997; 17:2336–2346. [PubMed: 9121483]

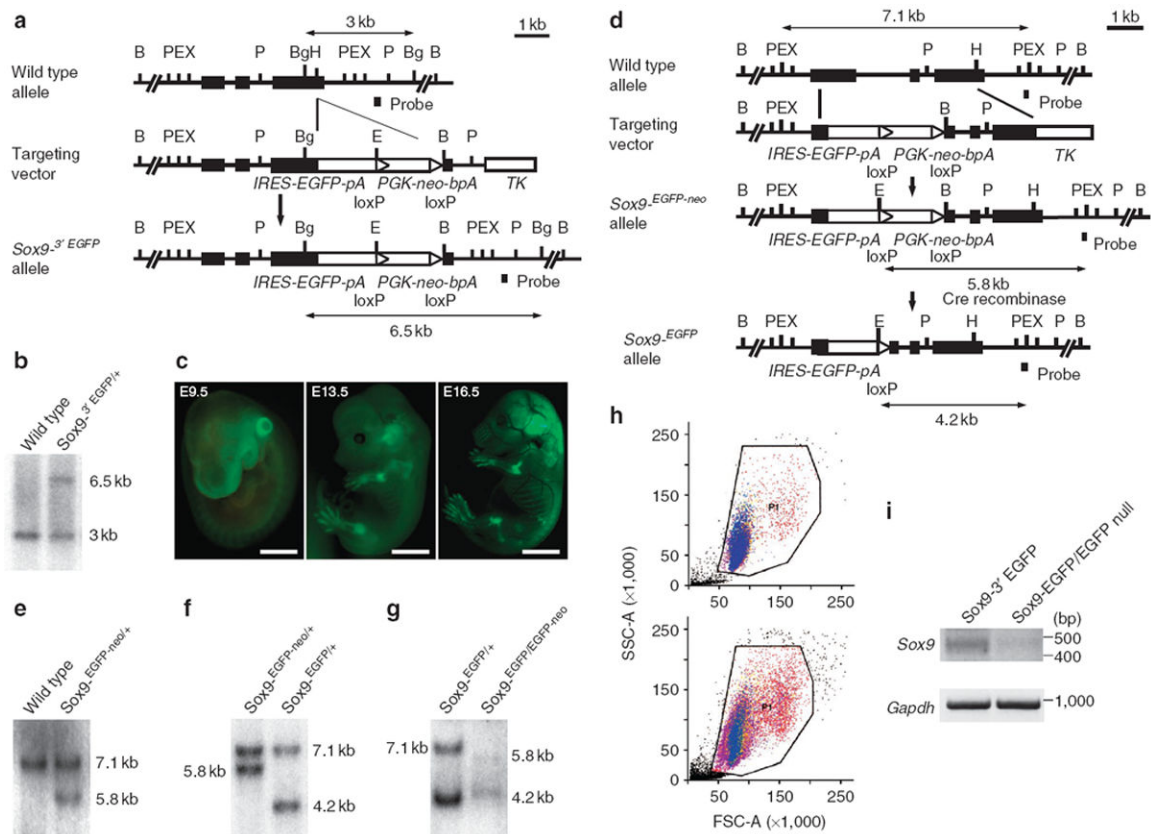


Figure 1. Generation of Sox9-3' EGFP knock-in mice and Sox9-EGFP/EGFP null chimeras
(a) The structure of the genomic *Sox9* locus, targeting vector and targeted allele for Sox9-3' EGFP knock-in mouse is indicated. Exons are depicted as closed boxes and intronic sequences are shown as solid lines. DNA fragments detected by Southern blot analysis are indicated by double arrows, with the restriction enzymes and the probe. The *IRES-EGFP-pA/loxP-flanked PGK-neo-bpA* cassette is depicted as open boxes. B, *Bam*HI; P, *Pst*1; E, *Eco*RI; X, *Xba*I; Bg, *Bgl*II; H, *Hpa*I. **(b)** Southern blot analysis of genomic DNA. Genomic DNA isolated from ES cell clones was digested with *Bgl*II and was then hybridized with the 3' probe. The wild-type and mutant alleles were detected as 3 kb and 6.5 kb fragments, respectively. **(c)** EGFP expression in E9.5, E13.5 and E16.5 Sox9-3' EGFP knock-in embryos. EGFP expression was detectable in a Sox9-specific pattern during embryogenesis. Scale bars, 500 μm (E9.5); 2 mm (E13.5) and 3 mm (E16.5). **(d)** The structure of the genomic *Sox9* locus, targeting vector and targeted allele for Sox9-EGFP/EGFP null chimera is indicated. DNA fragments detected by Southern blot analysis are indicated by double arrows. **(e)** Southern blot analysis of genomic DNA. Genomic DNA isolated from ES cell clones was digested with *Eco*RI and was then hybridized with the 3' probe. Wild-type and mutant alleles were detected as 7.1 kb and 5.8 kb fragments, respectively. **(f)** Southern blot analysis of the neo-deleted Sox9 EGFP clones after Cre recombination. The neo-deleted Sox9 EGFP allele was detected as a 4.2 kb fragment. **(g)** Southern blot analysis of the neo-deleted Sox9 EGFP/EGFP-neo clones. **(h)** Dot plot cytograms show enrichment of EGFP-positive cells in Sox9-3' EGFP knock-in embryos (top panel) and Sox9-EGFP/EGFP null chimeras (bottom panel). Only cells from a P1 population showing high green fluorescence

were sorted. (i) RT-PCR analysis of Sox9 expression using total RNA extracted from sorted EGFP-positive cells of Sox9-3' EGFP knock-in embryos and Sox9-EGFP/EGFP null chimeras.

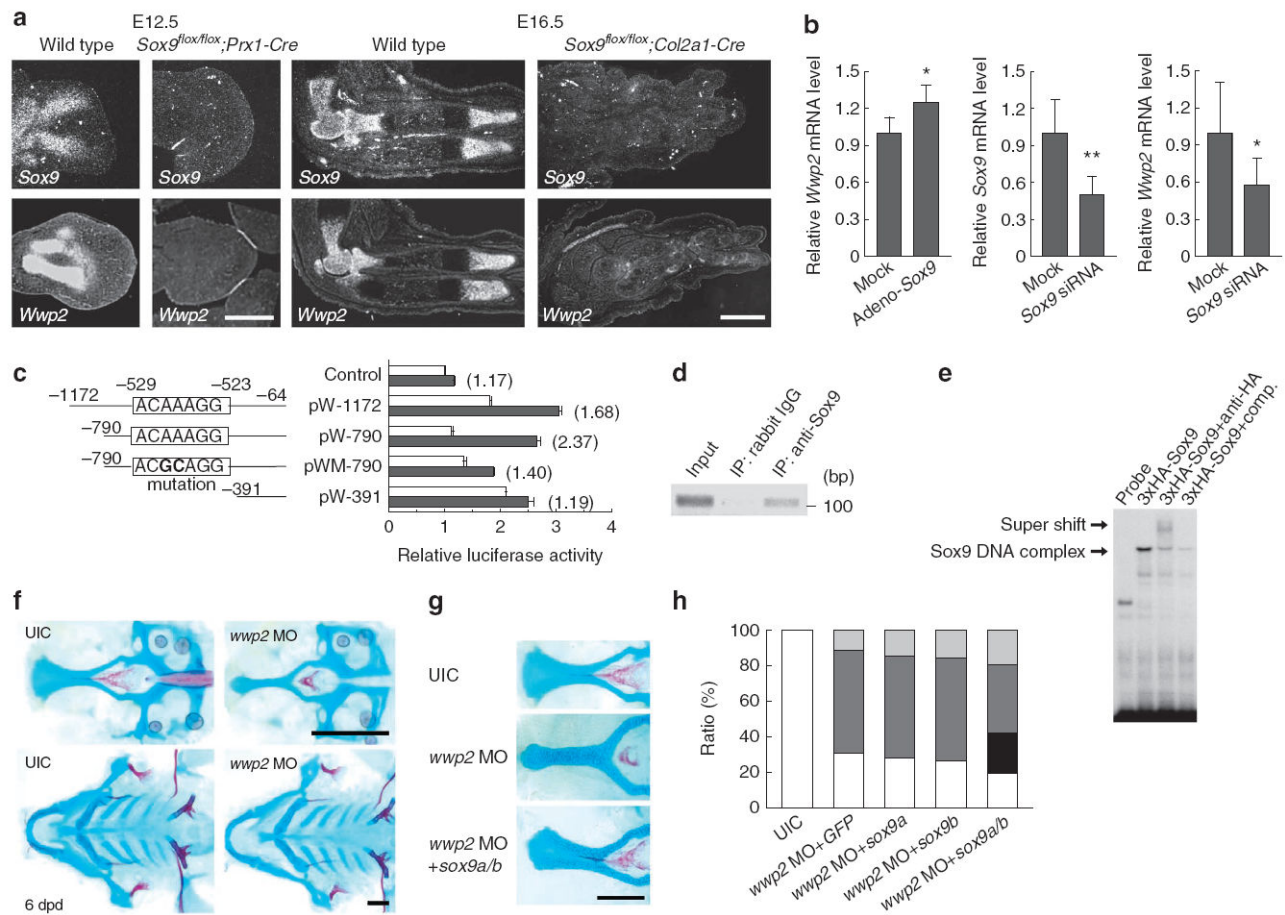


Figure 2. *Wwp2* is identified as a downstream target of *Sox9* and regulates palatogenesis (a) *In situ* hybridization of *Sox9* and *Wwp2* in limb buds of wild-type, *Sox9^{flx/flx}Prx1-Cre* (E12.5) and *Sox9^{flx/flx}Col2a1-Cre* (E16.5) mice. Scale bar, 500 μ m. (b) Analysis of *Wwp2* mRNA expression levels by quantitative RT-PCR (qRT-PCR) in ATDC5 cells. ATDC5 cells were infected with human *Sox9*-expressing adenovirus (left panel) or transfected with 150 nM of siRNA for *Sox9* (right panel; mean \pm s.d.; * P < 0.05; ** P < 0.01; n = 5). (c) Luciferase promoter analysis using truncated forms of the *Wwp2* promoter in the presence or absence of the *Sox9* expression vector. HEK293 cells were transfected with the pW₋₁₁₇₂ (nt -1172 to -64), the pW₋₇₉₀ (nt -790 to -64), the pW₋₃₉₁ (nt -391 to -64) or the pWM₋₇₉₀ plasmid, which includes a 2 bp substitution mutation, in the presence (black bars) or absence (white bars) of *Sox9* expression vector. The value in brackets represents the *Sox9*-dependent increase in ratio (mean \pm s.d.; n = 4). (d) The specific binding of *Sox9* to the *Wwp2* promoter element detected by ChIP assay using ATDC5 cells. DNA-protein complex was immunoprecipitated by anti-*Sox9* antibody. (e) EMSA revealed the specific binding of *Sox9* to the *Wwp2* promoter element. comp., competitor (unlabelled probe). (f) Small and fused palate in zebrafish carrying morpholino-mediated knockdown of *wwp2* at 6 dpf. Zebrafish embryos were stained with alcian blue and alizarin red. UIC, uninjected control; MO, morpholino-treated animals. Scale bar, 200 μ m. (g, h) RNA rescue experiments for *wwp2* knockdown in zebrafish using *sox9a* and/or *sox9b*. (g) Palatal malformation induced by *wwp2* knockdown was partially rescued by the co-injection of *sox9a* and *sox9b*. Scale bar,

100 μm . **(h)** Single injection of *sox9a* or *sox9b* did not rescue the palatal malformation induced by *wwp2* knockdown. UIC; $n = 51$, *wwp2* MO + *GFP*; $n = 142$, *wwp2* MO + *sox9a*; $n = 111$, *wwp2* MO + *sox9b*; $n = 109$, *wwp2* MO + *sox9a/b*; $n = 92$ (white, normal; black, partial rescue; dark grey, fused and/or small; light grey, death).

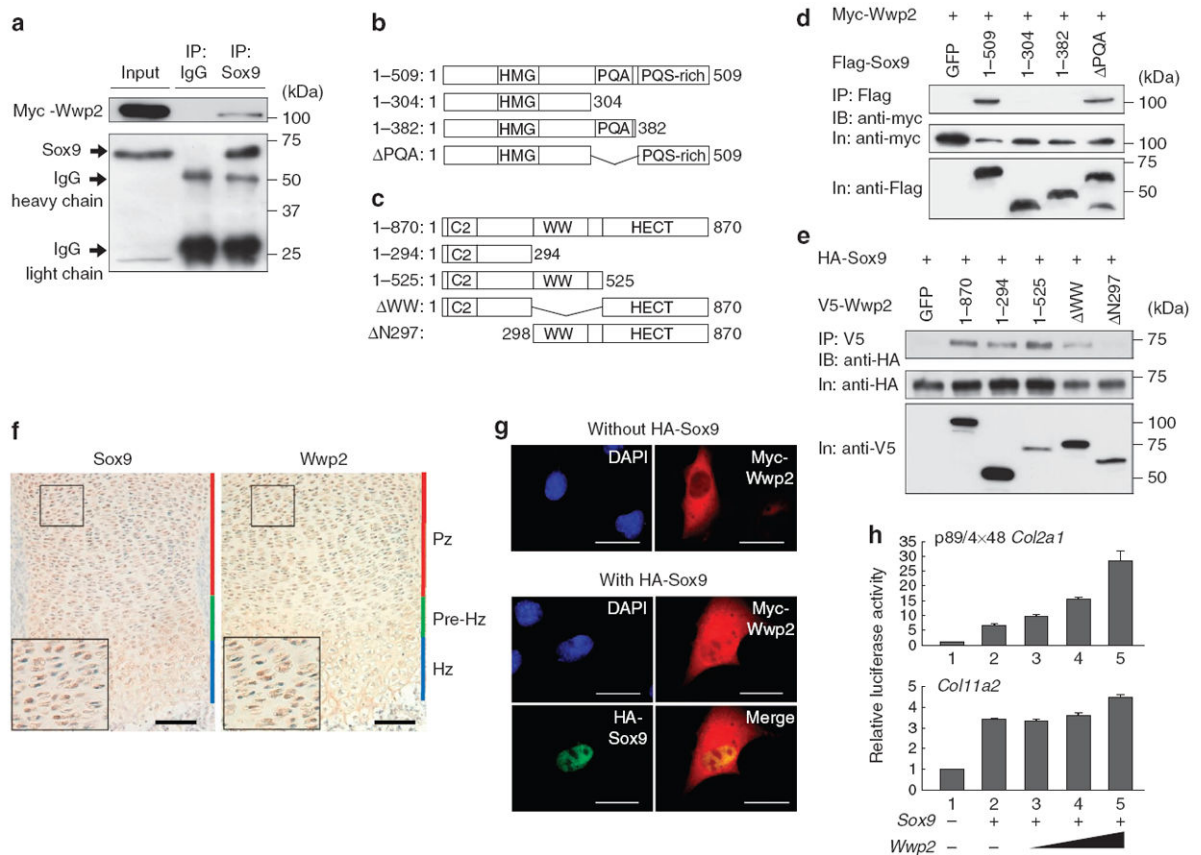


Figure 3. *Wwp2* activates *Sox9* by affecting its nuclear translocation

(a) *Wwp2* interacted physically with endogenous *Sox9* as demonstrated by IP assay using ATDC5 cells. Myc-tagged *Wwp2* was transfected into ATDC5 cells and total cell lysates were immunoprecipitated 48 h after transfection using rabbit IgG (negative control) or an anti-*Sox9* antibody, followed by immunoblotting with an anti-myc antibody. (b) Schematic images of *Sox9* deletion mutations. *Sox9* contains a high-mobility group domain (HMG, residues 104–182); a proline, glutamine and alanine domain (PQA, residues 339–379); and a proline, glutamine and serine-rich domain (PQS-rich, residues 402–509). (c) Schematic images of *Wwp2* deletion mutations. *Wwp2* contains a calcium-dependent membrane targeting domain (C2, residues 19–115), four tryptophan-based WW domains (WW, residues 300–477) and a carboxy terminus domain that is homologous to that of E6-AP (HECT, residues 525–870). (d) Co-immunoprecipitation assays between myc-tagged *Wwp2* and Flag-tagged deletion mutations of *Sox9*. GFP expression plasmid was used as a negative control. IB, immunoblotting; In, input. (e) Co-immunoprecipitation assays between HA-tagged *Sox9* and V5-tagged deletion mutations of *Wwp2*. GFP expression plasmid was used as a negative control. (f) Immunohistochemical analysis of *Sox9* and *Wwp2* in wild-type mouse limbs at E16.5 (DAB staining). Pz, proliferative zone; Pre-Hz, prehypertrophic zone; Hz, hypertrophic zone. Scale bar, 100 μ m. (g) Nuclear translocation of *Wwp2* in the presence or absence of exogenously overexpressed *Sox9* in C3H10T1/2 cells. The nuclear translocation of *Wwp2* was associated with *Sox9*. Scale bar, 20 μ m. (h) Luciferase reporter assay using the p89/4×48 *Col2a1* reporter plasmid or *Col11a2* reporter plasmid in

C3H10T1/2 cells. The reporter activities increased in a Wwp2 dose-dependent manner (mean \pm s.d.; $n = 5$).

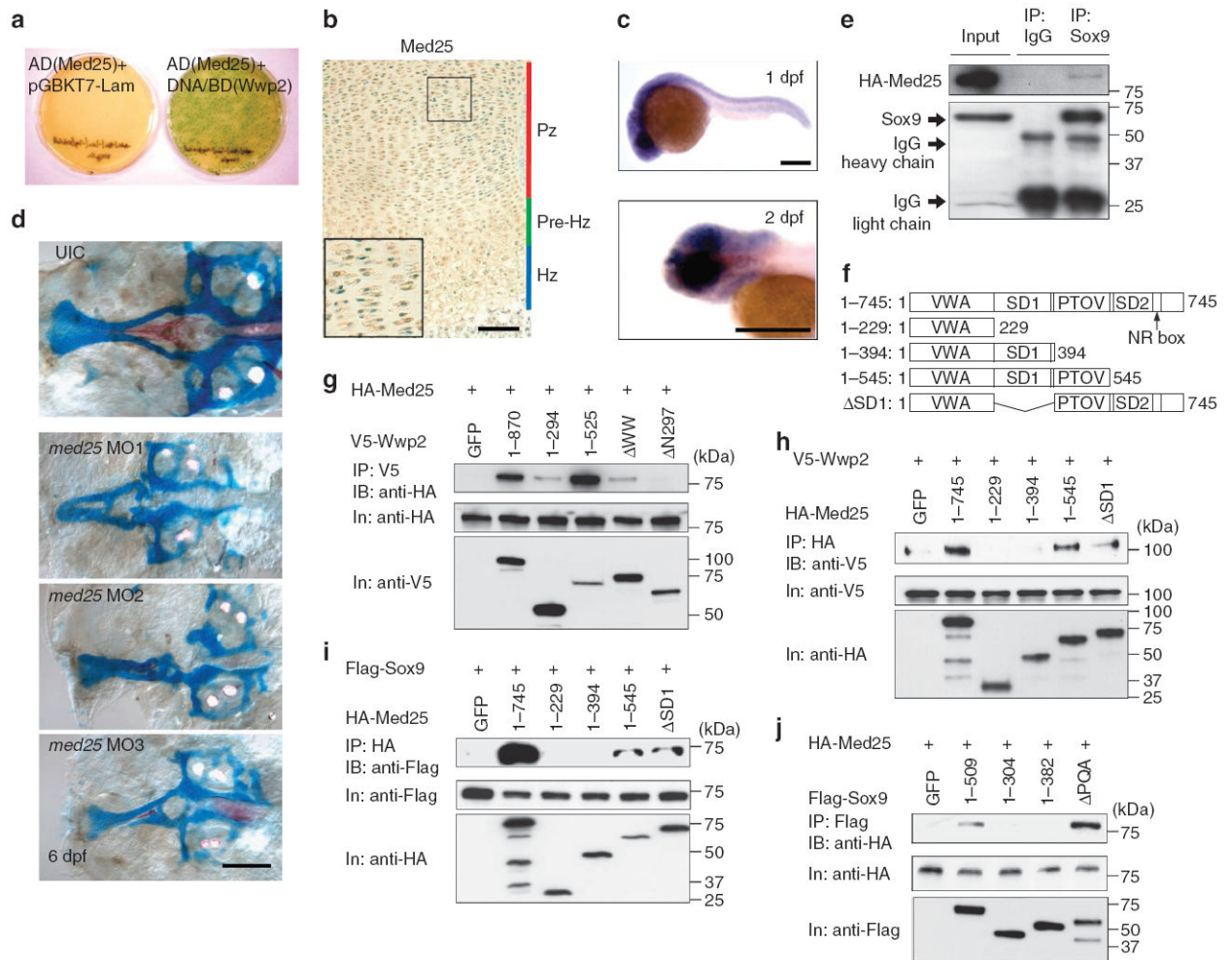


Figure 4. Med25 is involved in palatogenesis and interacts physically with Sox9 and Wwp2
(a) Verification of the physical interaction between Wwp2 and Med25 by a yeast two-hybrid assay. The AH109 yeast strain was co-transformed with the pGADT7 vector expressing full-length Med25 and the pGBKT7-Lam vector (negative control; left dish), or the pGBKT7 vector expressing full-length Wwp2 (right dish) was cultured on SD/– Ade/– His/– Leu/– Trp/X- α -Gal high-stringency plates. **(b)** Immunohistochemical analysis of Med25 in a wild-type mouse limb at E16.5 (DAB staining). Scale bar, 100 μ m. **(c)** Whole-mount *in situ* hybridization of *med25* in zebrafish at 1 dpf (top panel) and 2 dpf (bottom panel). Scale bar, 500 μ m. **(d)** Morpholino-mediated knockdown of *med25* in zebrafish induced palatal malformation. Three different kinds of palatal morphological malformations (*med25* MOs1–3) were observed. Scale bar, 100 μ m. **(e)** Med25 interacted physically with endogenous Sox9 detected by IP assay using ATDC5 cells. HA-tagged *Med25* was transfected into ATDC5 cells and a total cell lysate was immunoprecipitated 48 h after transfection using rabbit IgG (negative control) or an anti-Sox9 antibody, followed by immunoblotting with an anti-HA antibody. **(f)** Schematic images of Med25 deletion mutations. Med25 contains a von Willebrand factor type A domain (VWA, residues 1–228), a synapsin I domain 1 (SD1, residues 229–381), a conserved region found in prostate tumour overexpressed protein 1 domain (PTOV, residues 395–545), an SD2 domain (residues 554–731) and an NR box

(residues 646–650). **(g–j)** Co-immunoprecipitation assays using deletion mutations of Sox9, Wwp2 or Med25. GFP expression plasmid was used as a negative control. **(g)** Immunoprecipitation between HA-tagged full-length Med25 and V5-tagged deletion mutations of Wwp2. **(h)** Immunoprecipitation between V5-tagged full-length Wwp2 and HA-tagged deletion mutations of Med25. **(i)** Immunoprecipitation between Flag-tagged full-length Sox9 and HA-tagged deletion mutations of Med25. **(j)** Immunoprecipitation between HA-tagged full-length Med25 and Flag-tagged deletion mutations of Sox9.

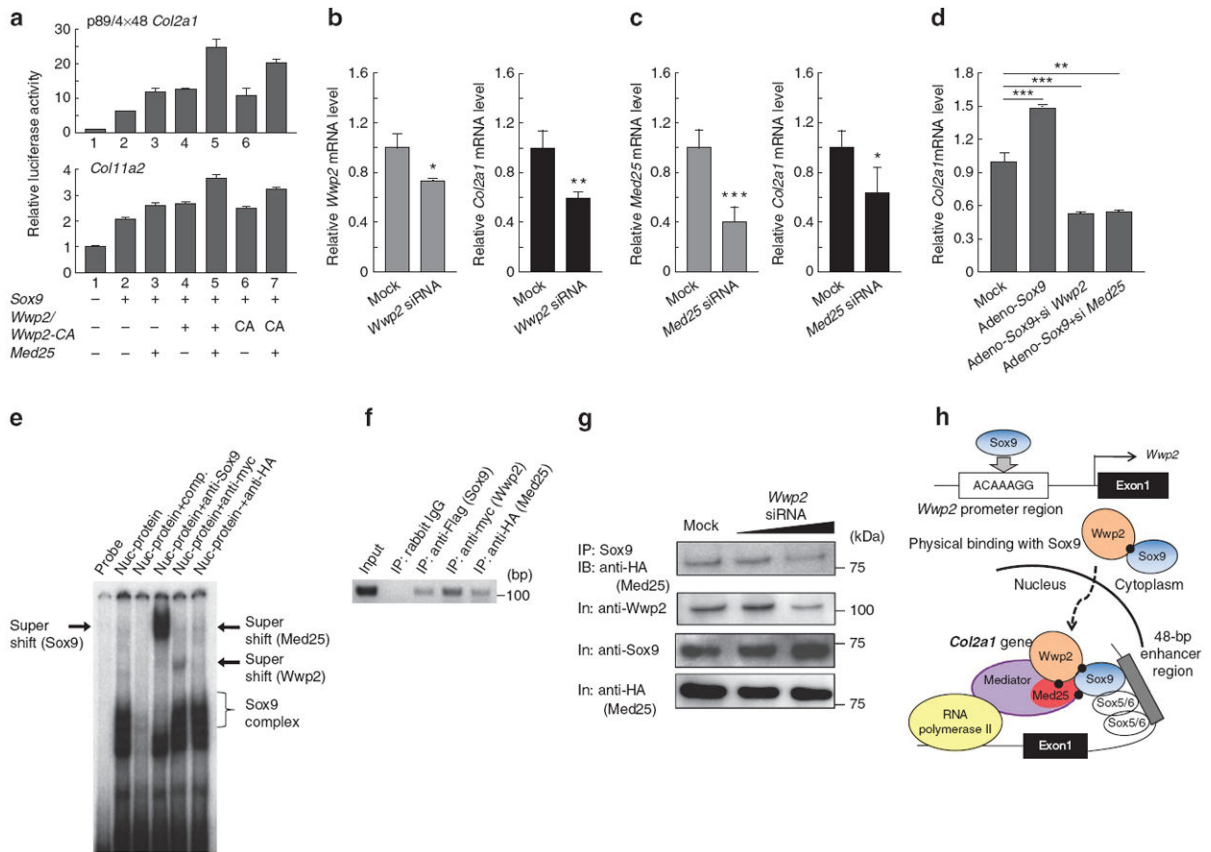


Figure 5. Wwp2 mediates formation of transcriptional complex with Sox9 and Med25 and regulates Sox9 transcriptional activity

(a) Luciferase reporter assay using the p89/4×48 *Col2a1* reporter and *Col11a2* reporter plasmid in C3H10T1/2 cells. *Wwp2-CA* includes a mutation in the HECT domain of *Wwp2*. (mean ± s.d.; $n = 5$). (b, c) Knockdown of *Wwp2* (b) or *Med25* (c) using siRNAs led to the downregulation of *Col2a1* transcription in C3H10T1/2 cells detected by qRT-PCR. (mean ± s.d.; * $P < 0.05$, ** $P < 0.01$, *** $P < 0.001$; $n = 4$). (d) Downregulation of *Col2a1* induced by knockdown of *Wwp2* or *Med25* in C3H10T1/2 cells was not restored by exogenous Sox9 overexpression. (mean ± s.d.; Dunnett's test, ** $P < 0.01$; *** $P < 0.001$; $n = 5$). (e) EMSA using nuclear protein from C3H10T1/2 cells that were co-transfected with Flag-tagged Sox9, myc-tagged *Wwp2* and HA-tagged *Med25*. The 48-bp *Col2a1* enhancer oligonucleotide probe was used. Nuc-protein, nuclear protein. (f) ChIP assay detected recruitment of Sox9, *Wwp2* and *Med25* to the chondrocyte-specific enhancer region of the *Col2a1* gene. Cell lysate extracted from C3H10T1/2 cells that were co-transfected with Flag-tagged Sox9, myc-tagged *Wwp2* and HA-tagged *Med25* was immunoprecipitated with antibodies for each tag. (g) Downregulation of *Wwp2* led to the attenuation of the physical binding between Sox9 and *Med25*. The *Wwp2* siRNA was initially transfected into ATDC5 cells and HA-tagged *Med25* was additionally transfected 24 h after transfection with *Wwp2* siRNA. Nuclear protein was immunoprecipitated with an anti-Sox9 antibody, followed by immunoblotting with an anti-HA antibody. (h) Model describing the mechanism underlying the physical and functional interaction between Sox9, *Wwp2* and *Med25*. Sox9 regulates the transcription of *Wwp2* and mediates the nuclear translocation of *Wwp2*, resulting in the

formation of a transcriptional complex, including RNA polymerase II and Sox 5/6, which regulates the expression of the *Col2a1* gene.